Theoretical and Computational Acoustics
D. Lee, Y-H Pao, M.H. Schultz, and Y-C Teng (Editors)

Geometrical Errors and Focalization in Matched Field Inversion for Geoacoustic Properties

N.R. Chapman
School of Earth and Ocean Sciences, University of Victoria
Victoria, B.C. Canada V8W 2Y2

K.S. Ozard and M.L. Yeremy
Esquimalt Defence Research Detachment
FMO Victoria B.C. Canada V0S 1B0

This paper investigates the effect of uncertainty in the geometrical parameters on the performance of matched field inversion for geoacoustic properties. The investigation is carried out using simulated data for a vertical line array. The results indicate that there is significant degradation in performance for small errors (1/3 wavelength) in range, ocean depth, and depth and tilt of the array. The relatively high sensitivity to mismatch in experimental geometry suggests that uncertainties of this type can be tolerated in the inversion by including the geometrical parameters in the global search algorithm. The simulations show that perfomance is improved by inverting for both the ocean bottom properties and the geometrical parameters simultaneoulsy.

1. Introduction

Matched Field (MF) inversion has been demonstrated to be an effective technique for estimation of geoacoustic properties of the ocean bottom.[1–3] In its simplest form, the concept is very straightforward: for a known experimental geometry, MF processing is used to invert measurements of the acoustic field at an array of sensors in order to determine the properties of the ocean waveguide. The inversion algorithm combines MF processing with a global search technique in order to investigate a multi-dimensional model parameter space. Two search methods have generally been employed: simulated annealing[1,2] and genetic algorithms,[3] and a combination of genetic algorithms and gradient descent has also been proposed.[4]

The performance of MF inversion is affected by many factors, including the components of the numerical algorithm such as the type of MF processor, the acoustic propagation model, and the form of the geoacoustic model, and experimental factors such as the data quality and uncertainty in the experimental geometry. Although the geometry is assumed to

be known, some degree of error always exists in the measurements made to define the source and receiver locations. Errors in the parameters that define the experimental configuration are manifested in the inversion as mismatch. In general, the inversion performance is sensitive to mismatch in quantities such as range, ocean depth, source depth, and array depth and tilt.

In this paper we investigate the effect of uncertainties in the experimental geometry on the performance of a MF inversion algorithm based on a Bartlett linear processor and a vertical line array (VLA). Inversions were carried out using modelled or replica fields that were calculated for known amounts of error in the geometrical parameters. The relatively high sensitivity to mismatch due to uncertainties in the experimental configuration suggests that the errors can be tolerated in the inversion by including the geometrical parameters in the global search process. This application of the concept of focalization[5] was investigated in the study.

In the remainder of this paper, the matched field inversion method is outlined and the environment for the simulation study is described. Following this, the results obtained for the effect of geometrical errors on inversion performance are presented, and the use of focalization as a means for tolerating and exploiting the errors is discussed.

2. Matched Field Inversion Method

The cost function, $B(m)$, for the MF inversion algorithm is based on the Bartlett MF processor, which describes the correlation between the measured and modelled acoustic fields. This function is defined as

$$B(m) = p^*(m)\, R\, p(m) \tag{2.1}$$

where $p(m)$ is the field calculated for a specific environmental model m, and R is the cross spectral matrix of the measured field, X. Although the Bartlett processor has low resolution and high sidelobes, it is robust to conditions of mismatch and noise, and is thus appropriate for searching the geoacoustic model parameter space. The replica fields were calculated using the normal mode model Krakenc.[6] This model calculates the discrete complex wavenumbers corresponding to the propagating modes in an elastic waveguide, and is suitable for the geoacoustic model used in this study.

The geoacoustic model consists of three homogenous layers: a water layer, a relatively thin fluid sediment layer, and an elastic basement half-space. The sediment is described by its density, sound speed, attenuation and layer thickness; the basement is described by the compressional and shear speeds and attenuations, and the density.

A simulated annealing algorithm was used to search the model parameter space in order to estimate the geoacoustic parameters. The search was initiated with random values selected within specific bounds for each model parameter; the imposed bounds were sufficiently large to span the expected range of values for the properties of the bottom materials. The inversion then proceeded through a series of iterations involving random perturbations of the model parameters while a control parameter, analogous to the temperature, was reduced. Perturbations that increased the cost function were accepted unconditionally; those

that decreased the cost function were accepted according to an acceptance probability given by the Boltzmann distribution,

$$P(\Delta E_i) = \exp\left(\frac{\Delta E_i}{s_i T}\right). \tag{2.2}$$

Here s_i is a scale factor for the ith model parameter and T is the control parameter. The scale factor accounts for the different sensitivities of the model parameters, so that all parameters converge at about the same rate in analogy with the cooling of a mixture.[1] The temperature was reduced according to the schedule given by

$$T_{j+1} = \gamma^{j+1} T_0, \text{ with } \gamma \leq 1 \text{ and } j = 0, 1, \ldots \tag{2.3}$$

The starting temperature, T_0, was determined by observing several short MF runs with different initial temperatures in order to select a value that provided sufficient freedom in the initial stages, analgous to a melted state. Previous work has indicated that an acceptance of 80-85% of all model perturbations corresponds to a sufficiently melted state. The number of iterations was estimated by calculating the temperature at which the acceptance criterion excluded any changes greater than a preset value of the tolerable error. The model parameter values were perturbed according to

$$m_{i+1} = m_i + \varepsilon^3 \, \delta_i \tag{2.4}$$

where ε is a random number from a uniform distribution on [-1,1], and δ_i is the maximum perturbation for the ith parameter.[1,2] This expression generates a reasonable approximation to a Cauchy distribution. It is generally more effective than a Gaussian schedule in searching the parameter space because it provides a greater chance of making large changes in parameter values, while at the same time ensuring that most changes are small.

3. Simulations

The simulations were carried out for a VLA in the ocean environment shown in Fig. (1). The sound speed profile for the water column was a North Pacific profile that was truncated at 1000 m. The geoacoustic bottom profile consisited of two layers: a sediment layer, h = 75 m, with density, $\rho_1 = 1.8$ g/cm^3, sound speed, $c_1 = 1600$ m/s, and attenuation, $\alpha_1 = 0.2$ dB/λ; and an elastic basement with density, $\rho_2 = 2.4$ g/cm^3, p-wave speed, $c_{2p} = 2700$ m/s, shear wave speed, $c_{2s} = 1250$ m/s, and both attenuations, $\alpha_{2p,s} = 0.2$ dB/λ. The VLA consisted of 16 hydrophones spaced at 40 m, with the topmost element at a depth of 200 m. The array was located 2 km from a 10 Hz source at a depth of 40 m. For these conditions, there were 14 modes. The Krakenc[6] solutions were benchmarked against SAFARI[7] calculations to confirm that the code was indeed satisfactory for this environment.

Initially the model parameter sensitivities were investigated in order to determine the temperature scale factors. Each parameter was tested separately, by calculating the cost function for selected values of the parameters over the allowed range, while all other parameters were fixed at their true values. A hierarchy of sensitivity was observed, with fluid

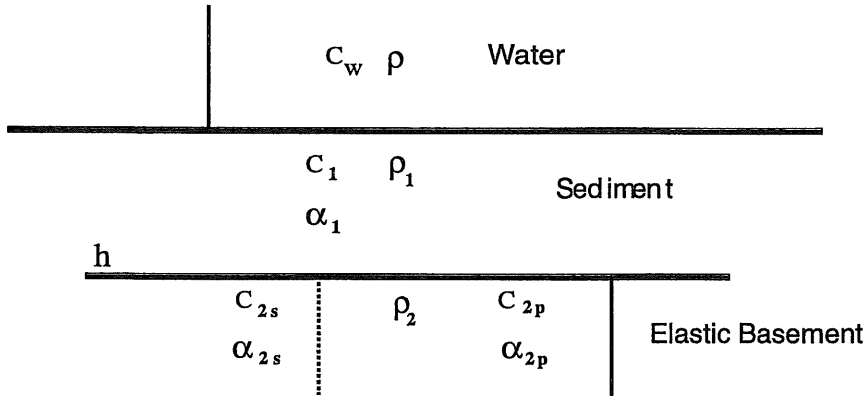

Fig. 1. The geoacoustic model for the simulations. The model is typical of thin sediment environments in the North Pacific.

layer depth and basement p-wave speed the most sensitive, followed by the sediment layer sound speed and basement s-wave speed. The least sensitive parameters were the densities and the attenuations. Similar tests carried out for the geometrical parameters indicated that the sensitivities for the range, ocean depth and array depth were equivalent to those for the most sensitive geoacoustic model parameters.

Based on the results of this study, the model parameters were assigned the scale factors shown in Table 1. The scale factors were held at fixed values throughout the inversion; experience has indicated that although the parameter sensitivites varied significantly from the initial to the final parameter set, the hierarchy of sensitivities was maintained during the annealing process. An inversion was carried out for the ideal case of no geometrical

Table 1. Results for ideal case: no geometrical errors.

Parameter	True	Limits	s	Estimate
h (m)	75	(50 - 100)	1.0	75.1
c_1 (km/s)	1.6	(1.5 - 1.7)	10.0	1.57
ρ_1 (g/cm^3)	1.55	(1.4 - 1.7)	100.0	1.64
c_{2p} (km/s)	2.7	(2.6 - 2.9)	1.0	2.71
c_{2s} (km/s)	1.25	(1.05 - 1.45)	10.0	1.26
ρ_2 (g/cm^3)	2.4	(2.1 - 2.7)	100.0	2.43

mismatch in order to verify the method. The annealing schedule for this inversion and all

the other tests reported here consisted of 10000 iterations, initiated with values of $T_0 = 10.0$, and $\gamma = 0.9988$. The final estimates for each parameter are listed in Table 1, along with the true values, the search range limits and the scale factors; all the attenuations were held fixed in the inversions. The final value of the Bartlett MF power was 0.9999, and the estimated values are in very close agreement with the true values; errors for even the less sensitive parameters are less than 2 %. The cooling curve is shown in Fig. (2), where the cost function for accepted models is plotted versus iteration number. There is roughly equal acceptance of increasing and decreasing models for about the first 4000 iterations, but subsequently the Bartlett MF power increases to a value close to unity.

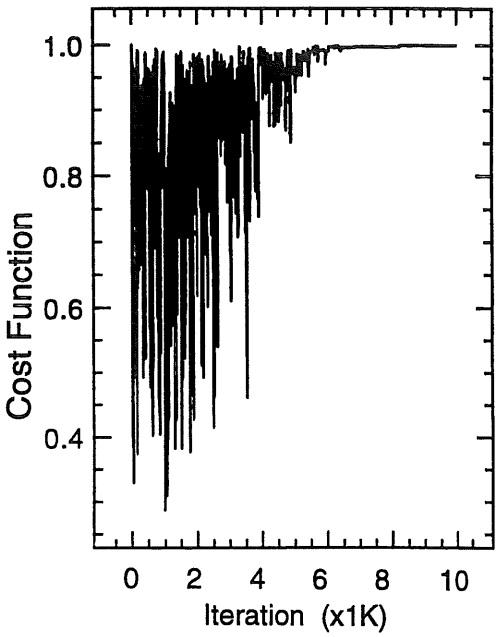

Fig. 2. Cost function for accepted models.

The investigation for the effect of mismatch in range was carried out by calculating simulated data for the true range, and then calculating replica fields for ranges that were displaced from the true range by a known fraction of the acoustic wavelength, λ. The results are shown in Table 2 for range errors of 1/3, 2/3 and 4/3 λ. The model parameter estimates are acceptable for the relatively small error of 1/3 λ, but for greater errors the cost function decreases significantly, and the errors in the most sensitive geoacoustic parameters are large (10 -20 %). This type of behaviour was observed for similar tests with all the other geometrical parameters.

The final column in Table 2 shows the effect of focalization. As discussed previously, focalization is applied in order to account for the uncertainty in the source-receiver distance in the inversion. The use of this approach is suggested because the sensitivity to range

Table 2. Effect of range errors.

Parameter	True Value	$1/3\lambda$	$2/3\lambda$	$4/3\lambda$	Range Search
h (m)	75	67.0	59.3	56.6	76.8
c_1 (km/s)	1.6	1.61	1.53	1.70	1.57
ρ_1 (g/cm^3)	1.55	1.62	1.68	1.63	1.64
c_{2p} (km/s)	2.7	2.75	2.89	2.89	2.69
c_{2s} (km/s)	1.25	1.10	1.26	1.12	1.24
ρ_2 (g/cm^3)	2.4	2.15	2.44	2.19	2.26
Range (km)	2.0				2.016
Cost Function		0.9527	0.8475	0.6465	0.9984

(as well as other geometrical parameters) is very high. Range was included as a search parameter, within the bounds ± 100 m ($2/3$ λ), and the inversion estimated both the geoacoustic parameters and the range simultaneously. All parameters, both geoacoustic and geometrical, were estimated accurately and the final Bartlett power is very close to unity, 0.9984.

Similar results were obtained using the concept of focalization to acount for errors in other geometrical parameters. A summary is presented in Table 3 for ocean depth, array depth and tilt, and also the range. The ocean depth was searched within the limits ± 100 m, the array depth within ± 20 m (half the hydrophone separation distance, $1/7$ λ), and the array tilt within $\pm 1.5°$ for a simulated tilt of 3°. In the table, the inversion performance for the geoacoustic parameters is summarized by the result for the most sensitive parameter, basement sound speed. For all cases, both types of parameters were estimated accurately, and the final Bartlett power was near unity.

Table 3. Effect of range errors.

Parameter	True Value	Limits	Estimate	c_{2p} (m/s)	Cost function
Range (km)	2.0	(1.9 - 2.1)	2.016	2690	0.9984
Ocean Depth (km)	1.0	(0.9 - 1.1)	0.999	2705	0.9996
Array Depth (m)	200	(180 - 220)	198.3	2684	0.9998
ArrayTilt (°)	3.0	(1.5 - 4.5)	3.14	2809	0.9994

4. Summary

The results of this simulation study indicate that matched field inversion performance is significantly degraded for relatively small errors in the experimental geometry. Errors as large as $1/3$ λ in some parameters can cause serious errors in the estimated values for the geoacoustic properties. However, since the sensitivity to the geometrical parameters

is relatively high, the concept of focalization provides a simple approach to account for geometrical uncertainties by inverting for both types of parameters simultaneously. The geometrical parameters were introduced into the global search process, and their values were searched over realistic limits for the experimental errors. The simulations show that significant improvement is obtained; the geoacoustic and geometrical parameters are estimated accurately, and the final Bartlett MF correlation is near unity.

References

1. M.D. Collins, W.A. Kuperman and H. Schmidt, "Nonlinear inversion for ocean-bottom properties," *J. Acoust. Soc. Am.* **92** (1992) 2770–2783.
2. N.R. Chapman and K.S. Ozard, "Matched field inversion for geoacoustic properties of young ocean crust, " in *Full Field Inversion Methods in Ocean and Seismo-Acoustics,* eds. O. Diachok, A. Caiti, P. Gerstoft and H. Schmidt, (Kluwer Academic Publishers, Dordrecht,) 1995, pp. 165-170.
3. D.F. Gingras and P. Gerstoft, "Global inversion of acoustic field data in shallow water using genetic algorithms," in *Full Field Inversion Methods in Ocean and Seismo-Acoustics,* eds. O. Diachok, A. Caiti, P. Gerstoft and H. Schmidt, (Kluwer Academic Publishers, Dordrecht,) 1995, pp. 317-322.
4. P. Gerstoft, "Inversion of acoustic data using a combination of genetic algorithms and the Gauss-Newton approach, " *J. Acoust. Soc. Am.* **97** (1995) 2181–2190.
5. M.D. Collins and W.A. Kuperman, "Focalization: Environmental focussing and source localization," *J. Acoust. Soc. Am.* **90** (1991) 1410–1422.
6. M.A. Porter and E.L. Reiss, "A numerical model for bottom interacting ocean acoustic normal modes, " *J. Acoust. Soc. Am.* **77** (1985) 1760–1767.
7. H. Schmidt, "SAFARI: Seismo-acoustic fast field algorithm for range independent environments," SACLANTCEN ASW Research Centre, San Bartolomeo, Italy, Memorandum SR–113, 1988.